Nonequilibrium Blunt-Body Flow Using the Method of Integral Relations

W C L Shih* and J R Baron†
Massachusetts Institute of Technology, Cambridge, Mass

The method of integral relations is extended to the problem of chemical coupling in nonequilibrium flow past an axisymmetric blunt body Choice of the integral method for such flows appears logical in view of its success for perfect gases and the inherent advantages of a direct method For the first approximation, no additional assumptions beyond those already made for the perfect-gas problem prove to be required In principle, only an additional statement as to the conservation of each reacting species is necessary Solutions for flow past a sphere using a five-component gas model composed of N_2, O_2, N, O, and NO are presented to show the variation of flow properties along the axial streamline and body surface The first approximation yields concentrations and temperatures immediately behind the shock, along the axial streamline, and on the body surface only Such properties may be determined within the flow field by performing a streamline calculation in conjunction with the first-approximation solutions The latter supply streamline geometries and behavior of pressure, density, and velocity along such paths A solution demonstrating the procedure is included Comparison of the present solutions with those based upon an inverse method shows reasonable agreement

Nomenclature

x = coordinate along body ($\xi = x$)
y = coordinate perpendicular to body ($\eta = y/\epsilon$)
θ = angle between body tangent and axis of symmetry
r_0 = perpendicular distance from axis to body, $r_0 = R_0 \cos\theta$
r = perpendicular distance from axis to general (x,y) point
R_0 = local radius of curvature of axisymmetric body
χ = shock angle relative to axis of symmetry
ϵ = shock detachment distance
ρ = density
p = pressure
u = velocity in x direction
v = velocity in y direction
h = enthalpy
q = total velocity, $(u^2 + v^2)^{1/2}$
T = temperature
M = Mach number
M_j = molecular weight of jth species
c_j = mass fraction of jth species, ρ_j/ρ
γ^0 = ratio of specific heats (freestream)
k^0 = $(\gamma^0 - 1)/2\gamma^0$
L' = a characteristic length
M^0 = either molecular weight of gas in freestream or freestream Mach number
$\bar{m}_0$ = initial mass fraction of oxygen = 0 2646
θ_{D_i} = normalized characteristic temperature for dissociation of ith molecule
θ_i = normalized characteristic vibrational temperature

Subscripts

n = normal to shock
t = total (stagnation quantities); or tangential to shock
1 = conditions immediately behind shock
0 = conditions on body surface
s = conditions on axial streamline
ψ = conditions along some streamline off the axis of symmetry
k = kth intermediate strip boundary
j = refers to species (O, O_2, N, N_2, or NO)

Superscripts

0 = freestream conditions
$'$ = dimensional quantities (also differentiation)
$*$ = conditions at singular point (sonic for equilibrium and frozen flow)
i = 0 (two dimensional), 1 (axisymmetric)

Received October 25, 1963; revision received February 28, 1964 This investigation was supported by the Department of the Navy, Bureau of Naval Weapons, under Contract NOw62-0765-d The authors wish to acknowledge R S Krupp for his contributions to a workable computer program

* Staff Member, Aerophysics Laboratory Student Member AIAA

† Associate Professor, Department of Aeronautics and Astronautics Associate Fellow Member AIAA

I Introduction

BLUNT bodies are extensively used to alleviate the high heat-transfer rates associated with hypersonic flight velocities For such speeds, the air flowing past the body cannot always be considered a perfect gas The perfect-gas assumption is customary for "low"-speed problems in which the kinetic energy of the flowing gas is insufficient to excite appreciably the internal degrees of freedom of the molecules At "high" velocities, a sufficient fraction of the freestream kinetic energy may be transformed into thermal energy by the bow shock wave, and vibration excitation, dissociation, ionization, etc , may become important It is the coupling between these phenomena and the usual flow processes which is most characteristic of the so-called real-gas effects and is responsible for the difficulties involved in analysis The fact that some number of particle collisions are required to bring the internal modes to equilibrium with the local translational temperature implies that a finite amount of time is required for the gas properties to achieve thermodynamic equilibrium The magnitude of this "relaxation" time (in general, a function of density, temperature, and species) relative to a characteristic flow time (e g , ratio of body length to velocity) is a measure of the departure from equilibrium of a flowing gas Consideration of real-gas effects in the subsonic region between the blunt body and its detached shock wave is the subject of this investigation In particular, the method of integral relations as discussed by Dorodnitsyn[1] and Belotserkovskii[2] and as summarized by Hayes and Probstein[3] is extended to include such effects in view of its relative straightforwardness, applicability to a variety of specified geometric shapes, and success in the prediction of flow-field behavior in the perfect-gas situation This approximate method also has the desirable feature that it may be extended to increasing degrees of accuracy For a real gas, the method requires reformula-

tion, since the extremely important simplification of isentropic streamlines no longer holds

Before a detailed discussion of this method is presented, mention should be made of existing techniques for the solution of the blunt-body problem Most of the following techniques are discussed by Hayes and Probstein [3] Three related techniques result in the Newtonian, constant-density, and thin-shock-layer solutions (Chaps 3–5 of Ref 3) The first is based upon the concept of an infinitesimally thin shock layer that is coincident with the body surface and with zero shear at the surface The latter two make use of the assumptions implied by their names to simplify the flow equations These solutions are very approximate representations of the true physical situation, although their justification is that they can provide some insight into the flow processes Both perfect-gas and real-gas solutions[4 5] using these assumptions have been performed Other approximate solutions include those obtained by an integral technique such as by Maslen and Moeckel[6] and by Belotserkovskii [2] The latter is the only technique which, in principle, may be extended to increasing degrees of accuracy as desired Thus far, the approximate methods discussed may all be considered a "direct" approach to the blunt-body problem, i e , a body is prescribed and the flow field and shock shape result from the solution The method of thin shock layers, however, may also be considered as an indirect method in which the shock-wave shape is prescribed and the corresponding body that supports this shock is sought In practice, of course, a direct approach is preferable

There also exist methods that yield "exact" solutions to the blunt-body problem They are exact in the sense that no mathematical approximations are required and the accuracy is limited only by the numerical techniques used These "exact" solutions include those of Gravalos,[7] Van Dyke,[3 8] and Garabedian and Lieberstein [3 9] The first is a streamtube iteration method (a direct method) that traces out streamtubes in the shock layer by satisfying the conservation equations along such tubes, although the convergence of this method is not clear The latter two schemes are indirect methods by which the flow equations are integrated from a prescribed shock wave and the body shape supporting this shock is obtained as the solution Although all of these schemes were formulated, initially, for a perfect gas, the streamtube method has been extended to real gases in equilibrium[10]; Lick[11 12] and Hall, Eschenroeder, and Marrone[13] have extended the indirect method of Van Dyke to include finite rate processes

II Formulation of the Problem

2 1 Basic Flow Equations

Assume an axisymmetric flow, normalized lengths with respect to a characteristic length (say L'), and similarly normalized pressure, density, temperature, enthalpy, and velocity components with respect to freestream stagnation values and the maximum speed, $(2h_t'^0)^{1/2}$ The steady flow of an adiabatic, inviscid, non-heat-conducting real gas is then governed by the following equations:

$$\frac{\partial}{\partial x}(\rho u r^i) + \frac{\partial}{\partial y}\left[\rho v r^i\left(1 + \frac{y}{R_0}\right)\right] = 0 \qquad (2\,1)$$

$$\frac{u}{1 + y/R_0}\frac{\partial u}{\partial x} + v\frac{\partial u}{\partial y} + \frac{uv}{(1 + y/R_0)R_0} + \frac{k^0}{\rho(1 + y/R_0)}\frac{\partial p}{\partial x} = 0 \qquad (2\,2)$$

$$\frac{u}{(1 + y/R_0)}\frac{\partial v}{\partial x} + v\frac{\partial v}{\partial y} - \frac{u^2}{(1 + y/R_0)R_0} + \frac{k^0}{\rho}\frac{\partial p}{\partial y} = 0 \qquad (2\,3)$$

$$h + q^2 = 1 \qquad (2\,4)$$

$$\frac{\rho u}{1 + y/R_0}\frac{\partial c_j}{\partial x} + \rho v\frac{\partial c_j}{\partial y} = \frac{L'}{q_{max}'^0\rho_t'^0}K_j \qquad (j = O, O_2, \quad) \qquad (2\,5)$$

The equations are written for an orthogonal curvilinear coordinate basis measured along and normal to the body (Fig 1) A prime denotes a dimensional quantity, and K_j is the net rate of production of the jth species Equations (2 1–2 4) are of the same form as the usual inviscid perfect-gas equations, whereas, because of the possibility of chemical reactions, a statement (2 5) must be made as to the conservation of each reacting species The coupling of (2 5) with (2 1–2 4) is implicit from the dependence of the latter upon the complex physical properties description of the medium

Air will be the working medium with the number of reaction equations dependent upon the number of chemical reactions and the species formed For the present, only $j = O_2, N_2, O, N$, and NO are considered as constituents; thus three rate equations are required along with two algebraic relations stating conservation of nitrogen and oxygen in proper proportions for air The latter two are

$$c_O + c_{O_2} + c_N + c_{N_2} + c_{NO} = 1 \qquad (2\,6)$$

$$c_O + c_{O_2} + (M_O/M_{NO})c_{NO} = \bar{m}_0 \qquad (2\,7)$$

where c_j is the mass fraction of the jth specie, and $\bar{m}_0$ is the net mass fraction of oxygen present (taken to be 0 2646) The latter varies, depending on the initial composition of the gas used Vibrations will be assumed in equilibrium, although, in principle, vibrational relaxation effects may be studied by including vibration rate equations for O_2, N_2, and

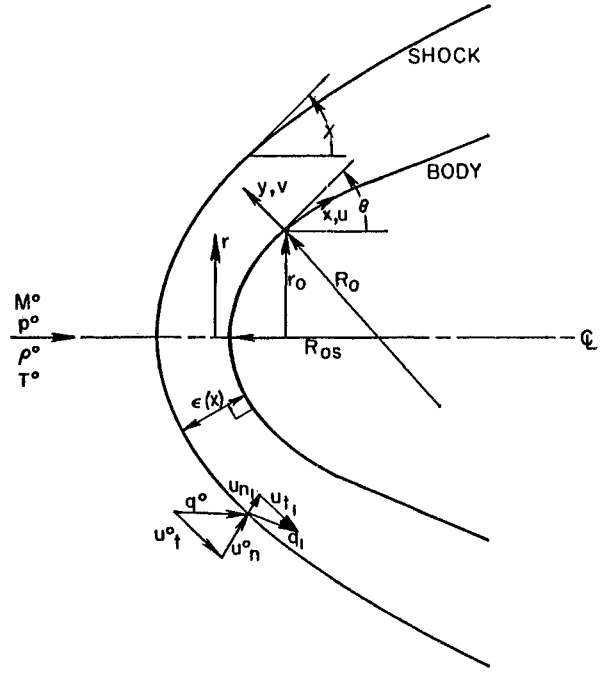

Fig 1a Coordinate system

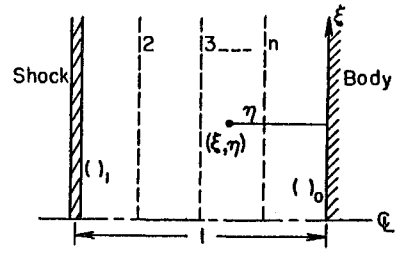

Fig 1b Normalized coordinates

NO Until recently, such relations have been assumed as linearized forms that do not account for vibration-dissociation coupling[14–16] and may indeed lead to physically erroneous results In view of some question about a proper description of the vibrational coupling, the vibrational equilibrium model was deemed sufficient to describe the salient features of the flow phenomena

An equation of state and Eqs (2 1–2 7) plus appropriate boundary conditions completely specify the blunt-body nonequilibrium flow problem

2 2 Boundary Conditions

Since the body is a streamline, the condition for tangential flow on the body is

$$v_0 = 0 \tag{2 8}$$

and the Rankine-Hugoniot relations are satisfied at the shock:

Continuity

$$\rho^0 u_n{}^0 = \rho_1 u_{1n} \tag{2 9}$$

Momentum

$$\rho^0 u_n{}^{0^2} + k^0 p^0 = \rho_1 u_{1n}{}^2 + k^0 p_1 \text{ (normal)} \tag{2 10}$$

$$u_t{}^0 = u_{1t} \qquad \text{(tangential)} \tag{2 11}$$

Energy

$$u_n{}^{0^2} + h^0 = u_{1n}{}^2 + h_1 \tag{2 12}$$

Where the relations between u_{1n} and u_{1t} and velocities in the present coordinate system are given by

$$u_1 = u_{1t}\cos(\chi - \theta) + u_{1n}\sin(\chi - \theta)$$

$$u_{1t} = u_t{}^0 = q^0 \cos\chi$$

$$v_1 = u_{1t}\sin(\chi - \theta) - u_{1n}\cos(\chi - \theta)$$

$$u_n{}^0 = q^0 \sin\chi$$

The thickness of the shock is of the order of a few mean free paths Since relaxation effects are due to many-collision processes, it is assumed that the gas state is frozen in passing through the shock, except for contributions from the vibrational mode Thus, immediately behind the shock, the concentrations are

$$(c_O)_1 = (c_N)_1 = (c_{NO})_1 = 0$$

$$(c_{O_2})_1 = \bar{m}_0 \qquad (c_{N_2})_1 = 1 - \bar{m}_0$$

and the normalized vibrational energies as defined later are

$$e_j(T) = e_j(T_1) \qquad (j = O_2, N_2, NO) \tag{2 13}$$

In some situations (e g , a hypersonic test facility), conceivably the oncoming stream may not be in equilibrium This may be partially accounted for by assigning an effective value of γ^0 corresponding to a certain level of dissociation in a frozen freestream The boundary condition behind the shock then corresponds to a frozen shock with the initial dissociation level no longer zero

Finally, a relation is required to relate the shock inclination angle χ to detachment distance ϵ From Fig 1, the geometry indicates that

$$d\epsilon/dx = [1 + (\epsilon/R_0)]\tan(\chi - \theta) \tag{2 14}$$

2 3 Gas Model

Details of the gas model are not included, since many papers are available which present these adequately Specifically, the reaction rates are from Ref 17, and the equilibrium expressions are derived in a straightforward manner from statistical mechanical considerations The specific reactions describing the high-temperature regime for the five-component gas model are (with $M = O_2, O, N_2, N, NO$)

$$O_2 + M \rightleftarrows 2O + M \tag{2 15}$$

$$N_2 + M \rightleftarrows 2N + M \tag{2 16}$$

$$NO + M \rightleftarrows N + O + M \tag{2 17}$$

$$O_2 + N \rightleftarrows NO + O \tag{2 18}$$

$$N_2 + O \rightleftarrows NO + N \tag{2 19}$$

$$N_2 + O_2 \rightleftarrows 2NO \tag{2 20}$$

Such reactions do not have equal importance in different flow regimes Subreactions of (2 15) and (2 16) occur because some particles are more efficient than others for inducing dissociation or recombination Equations (2 15–2 20) are considered to be a reasonable description of the reaction processes if ionization is excluded

2 4 Method of Integral Relations

For the perfect-gas case, only Eqs (2 1) and (2 3) are required, since one momentum relation is furnished by the integrated Bernoulli equation and the energy equation is equivalent to entropy conservation along streamlines The entropy level thus depends only on the stream function Equation (2 3) may be cast into divergence form After dividing the shock layer into strips of equal width, Eqs (2 1) and (2 3) may be integrated outward from the body to each strip boundary successively at some constant value of x The procedure results in a set of total differential equations if the distribution of certain sets of dependent variables is assumed to be known across the shock layer Dorodnitsyn[1] made the suggestion that interpolation polynomials be used to approximate the various distributions across the shock layer In principle, then, one may adjust the chosen number of strips to achieve the desired accuracy, i e , with increasing number of strips, the more closely actual distributions may be represented across the shock layer However, Belotserkovskii has shown that the linear approximation (that is, one strip bounded by body and shock) gives good results relative to experimental data for shock shape of a circular cylinder and flow properties along the body surface In addition, agreement between solutions for the second and third approximations implies convergence

It is convenient to distort the shock layer into rectangular form by means of the following coordinate transformation; let

$$\xi = x \tag{2 21}$$

$$\eta = y/\epsilon \tag{2 22}$$

such that

$$\frac{\partial}{\partial x} = \frac{\partial}{\partial \xi} - \frac{\eta}{\epsilon}\frac{\partial \epsilon}{\partial x}\frac{\partial}{\partial \eta} \tag{2 23}$$

$$\partial/\partial y = (1/\epsilon)(\partial/\partial\eta) \tag{2 24}$$

The region of interest in the (ξ,η) plane is bounded by the body, shock, and stagnation streamline and corresponds to the intervals $0 \leq \eta \leq 1$ and $0 \leq \xi$ (Fig 1b) Solutions may be extended past the sonic point into the supersonic region[18] or alternatively used to determine flow properties within the subsonic cap as initial conditions for a subsequent method of characteristics

Following Belotserkovskii, the region of Fig 1b is divided into N strips and Eqs (2 1–2 3 and 2 5) are transformed, put in divergence form, and integrated successively along ξ = const, from $\eta = 0$ to the boundary of each strip, $\eta_k = (N - k + 1)/N$ for $k = 1, 2, 3 \quad N$ The x momentum and reaction equations have been omitted, since, for the present, only the first approximation will be considered, and these equations then take on especially simple forms Performing

the integration and using Leibniz's rule for differentiating under an integral, (2 1) and (2 3) become, respectively,

$$\frac{d}{d\xi}\int_0^{\eta_k}(\rho u r^i)d\eta + \frac{1}{\epsilon}\frac{d\epsilon}{dx}\int_0^{\eta_k}(\rho u r^i)d\eta + \frac{1}{\epsilon}\left[(\rho v r^i)_k\left(1+\frac{\epsilon\eta_k}{R_0}\right)\right] - \frac{1}{\epsilon}\frac{d\epsilon}{dx}\eta_k(\rho u r^i)_k = 0 \quad (2\,25)$$

$$\frac{d}{d\xi}\int_0^{\eta_k}(\rho u v r^i)d\eta + \frac{1}{\epsilon}\left[\{(k^0 p + \rho v^2)r^i\}_k\left(1+\frac{\epsilon\eta_k}{R_0}\right)\right] - \frac{1}{\epsilon}(k^0 p + \rho v^2)_0 r_0{}^i + \frac{1}{\epsilon}\frac{d\epsilon}{dx}\int_0^{\eta_k}(\rho u v r^i)d\eta - \frac{1}{\epsilon}\frac{d\epsilon}{dx}\eta_k(\rho u v r^i)_k - \frac{1}{R_0}\int_0^{\eta_k}[(k^0 p + \rho u^2)r^i]d\eta - ik^0\cos\theta\int_0^{\eta_k} p\left(1+\frac{\epsilon\eta}{R_0}\right)d\eta = 0 \quad (2\,26)$$

Evaluation of the integrals requires integrands of known functions of η, and, since this involves precisely the sought properties, some approximations must be made Let us represent each integrand by $f_n(\xi,\eta)$, where $n = 1, 2,$, such that each integrand is of the form

$$f_n(\xi,\eta) = \sum_{m=0}^{N} a_{mn}(\xi)\eta^m \quad (2\,27)$$

Thus

$$\int_0^{\eta_k} f_n d\eta = \sum_{m=0}^{N} a_{mn}(\xi)\frac{1}{m+1}\eta_k{}^{m+1}$$

$$\frac{d}{d\xi}\int_0^{\eta_k} f_n d\eta = \sum_{m=0}^{N}\frac{da_{mn}}{d\xi}\frac{1}{m+1}\eta_k{}^{m+1} \quad (2\,28)$$

The specific integrands $f_n(\xi,\eta)$ requiring such representations in Eqs (2 25) and (2 26) are

$$\begin{matrix}(\rho u r^i) & p[1+(\epsilon\eta/R_0)] \\ (k^0 p + \rho u^2)r^i & (\rho u v r^i)\end{matrix} \quad (2\,29)$$

Of course, for higher approximations, the terms $(\rho u c_j)$ and $(L'/q_{\max}{}^{0'}\rho_t{}^{0'})K_j$ must be included, since the Bernoulli and simple rate equations can no longer be used

Depending on the number of strips N, certain of the a_{mn}'s will be evaluated at the strip interfaces, and it is clear that substitution of (2 27) and (2 28) into (2 25) and (2 26) results in total differential equations in ξ along the strip interfaces

2 5 First Approximation

Although the formulation for the N-strip approximation has been presented, the complexity of the problem in practice increases greatly with N Since the $N = 1$ perfect-gas problem yields quite reasonable results, we shall consider the one-strip case to study the effects of relaxation on flow properties along the body surface When and if more accurate detail is desired for the flow field, more strips may be required

For the first approximation, a set of total differential equations is obtained along the body in terms of parameters evaluated at the shock Since the body is a streamline, exact forms of the x momentum and reaction equations are used without approximation For a sphere, the final set of differential equations for the one-strip approximation are

$$\rho_0\epsilon\sin\xi\left[1-\frac{u_0{}^2}{k^0(dp_0/d\rho_0)}\right]\frac{du_0}{d\xi} + b\frac{d\chi}{d\xi} + c\frac{d\epsilon}{d\xi} + d = 0 \quad (2\,30)$$

$$k^0(dp_0/d\xi) + \rho_0 u_0(du_0/d\xi) = 0 \quad (2\,31)$$

$$e(d\chi/d\xi) + f(d\epsilon/d\xi) + g = 0 \quad (2\,32)$$

$$h_0 + u_0{}^2 = 1 \quad (2\,33)$$

$$\rho_0 u_0(dc_{O_0}/d\xi) = K_O \quad (2\,34a)$$

$$\rho_0 u_0(dc_{N_0}/d\xi) = K_N \quad (2\,34b)$$

$$\rho_0 u_0(dc_{NO_0}/d\xi) = K_{NO} \quad (2\,34c)$$

$$c_O + c_{O_2} + c_N + c_{N_2} + c_{NO} = 1 \quad (2\,34d)$$

$$c_O + c_{O_2} + (M_O/M_{NO})c_{NO} = \bar{m}_O \quad (2\,34e)$$

$$p = \rho T M^0\Sigma(c_j/m_j) \qquad (j = O_2, N_2, NO, O, N) \quad (2\,35)$$

$$h = M^0 T\sum_{i=O_2\ N_2\ NO}\frac{c_i}{m_i} + \frac{5}{7}M^0 T\sum_{i=O\ N}\frac{c_i}{m_i} + \sum_{i=O_2\ N_2\ NO}\frac{c_i}{m_i}e_{v_i} + \sum_{i=O_2\ N_2}\frac{D_i}{M_i}[(c_i)_1 - c_i] - \frac{D_{NO}}{M_{NO}}c_{NO} \quad (2\,36)$$

where

$$e_{v_i} = \frac{(2M^0/7)\theta_i}{\exp(\theta_i/T_i) - 1} \qquad D_i = \frac{2M^0}{7}\theta_{D_i}$$

and at equilibrium, $T_i = T$

The species production terms K_j are obtained by considering the sum of the net production of jth species by each of the reactions (2 15–2 20) [17] The coefficients in (2 30) and (2 32) are, in detail,

$$b = \epsilon(1+\epsilon)\left[\frac{\partial\rho_1 u_1}{\partial\chi} + \frac{\partial\rho_1 u_1}{\partial\xi}\frac{d\xi}{d\chi}\right]\sin\xi$$

$$c = (\rho_0 u_0 - \rho_1 u_1)\sin\xi$$

$$d = \epsilon(\rho_1 u_1 + \rho_0 u_0)\cos\xi + \epsilon^2\rho_1 u_1\cos\xi + 2(1+\epsilon)^2\rho_1 v_1\sin\xi$$

$$e = \epsilon(1+\epsilon)\left[\frac{\partial\rho_1 u_1 v_1}{\partial\chi} + \frac{\partial\rho_1 u_1 v_1}{\partial\xi}\frac{d\xi}{d\chi}\right]\sin\xi$$

$$f = -\rho_1 u_1 v_1\sin\xi$$

$$g = (1+\epsilon)[\{2k^0(p_1 - \rho_0) - [\epsilon\rho_0 u_0{}^2/(1+\epsilon)] - \epsilon\rho_1 u_1{}^2 + 2(1+\epsilon)\rho_1 v_1{}^2\}\sin\xi + \epsilon\rho_1 u_1 v_1\cos\xi]$$

The characteristic length L' has been taken to be the sphere radius R_0', and boundary conditions are given by Eqs (2 8–2 13) It is interesting to note that, as a result of using the exact forms of the x momentum and reaction equation, the total number of approximations required is the same as that used by Traugott[18] in the identically frozen case The details of the flow field between shock and body, however, are not completely specified, and an additional scheme (described below) must be employed for such evaluations In the multistrip problem, the strip interfaces are no longer streamlines, and Eqs (2 2) and (2 5) must be used in their entirety A singularity that effectively "determines" the initial shock detachment distance is apparent in Eq (2 30) When $u_0{}^2 = k^0(dp_0/d\rho_0)$, the surface velocity gradient becomes infinite unless the remaining terms are zero; a proper choice for ϵ removes the indeterminancy Indeed, in the perfect-gas and identically equilibrium cases, this critical u_0 value is merely the sonic point on the body In nonequilibrium flows, the process is no longer isentropic, and the interpretation of a sonic point no longer follows

In order to initiate the integration of Eqs (2 30–2 36), the initial gradient of u_0 must be known at the stagnation point (i e , symmetry axis, $\xi = 0$) Since all equations reduce to zero identities at that point, a limiting process may be applied

to Eqs (2 30) and (2 32) to yield (along $\xi = 0$ axis)

$$\epsilon \rho_0 (du_0/d\xi) + \epsilon \rho_1 (1 + \epsilon)(du_1/d\xi) + (1 + \epsilon)^2 \rho_1 v_1 = 0 \quad (2\,37)$$

$$\epsilon \rho_{1s} v_{1s} (du_1/d\xi) + (1 + \epsilon)\rho_1 v_1^2 + k^0(p_1 - p_0) = 0 \quad (2\,38)$$

However, since chemical reactions occurring at a finite rate are nonisentropic, still another relation is required to determine the stagnation-point pressure For this purpose, consider the limiting form of (2 1) in the (ξ,η) plane when specialized to the axial streamline:

$$2\epsilon \rho (\partial u/\partial \xi) + (1 + \epsilon\eta)(\partial/\partial\eta)(\rho v) + 2\epsilon \rho v = 0 \quad (2\,39)$$

Although Eq (2 37) is an approximate form of the continuity equation on the $\xi = 0$ axis, (2 38) is exact Using the two equations independently implies using one of the approximations (2 27) Still an additional expression is needed for $\partial u/\partial\xi$; this is obtained from the approximation used for (ρur) when specialized to the stagnation streamline From (2 27),

$$\rho ur = (\rho ur)_0 + [(\rho ur)_1 - (\rho ur)_0]\eta \quad (2\,40)$$

so that on the stagnation streamline

$$\rho_s \frac{\partial u_s}{\partial \xi} = \frac{\rho_{0s}}{1 + \epsilon\eta} \frac{\partial u_{0s}}{\partial \xi} + \left\{ \frac{1 + \epsilon}{1 + \epsilon\eta} \rho_1 \frac{\partial u_1}{\partial \xi} - \frac{\rho_0}{1 + \epsilon\eta} \frac{\partial u_{0s}}{\partial \xi} \right\} \eta \quad (2\,41)$$

In addition, Eqs (2 33–2 36) evaluated along the stagnation streamline are required These equations are sufficient to specify the stagnation conditions Thus, the first approximation for the nonequilibrium blunt-body problem is completely specified by Eqs (2 30–2 41), boundary conditions (2 8–2 13), and the thermodynamic relations

2 6 Flow-Field Calculations

It has been noted that no additional assumptions are required beyond those for a perfect-gas one-strip formulation This results since, in a one-strip formulation, differential equations are required only along the body, permitting the use of the exact form of the rate equations along both the body and stagnation streamline However, as a result, the present formulation yields values for p, ρ, u, and v throughout the shock layer but concentrations only along the stagnation streamline, body surface, and immediately behind the shock The rate equation along the body serves only to weight the flow-field properties (p, ρ, u, and v) differently from that of a perfect gas Thus, for concentrations *within* the flow field an additional scheme is proposed

Briefly, one may proceed as follows: the present solutions provide three relations for p, ρ, u, and v in the shock layer A streamline can be traced starting from the shock by means of a mass flow balance Using the three equations for p, ρ, u, and v, along with the differential Bernoulli equation, the rate equations may be integrated step by step along the streamline to yield the concentrations

Actually, there are several methods available for calculating the flow field due to the excess information introduced by the relations (2 27) for p, ρ, u, and v, i e , the quantities (ρur), (ρuvr), $(k^0p + pu^2)r$, and $p(1 + \epsilon\eta)$ From Eq (2 26) we observe that, for the first approximation, the last two integrals may be combined Although the results along the body are unaffected in any case, this does permit some freedom as to which set of integrands are linearized, namely, either the set (ρur), (ρuvr), $(k^0p + \rho u^2)r$, and $p(1 + \epsilon\eta)$ or the set (ρur), (ρuvr), and $[(k^0p + \rho u^2) + p(1 + \epsilon\eta)k^0 \cos\theta]$ The first set yields four equations in four unknowns and the latter three equations in four unknowns

For streamline integration, specification of the differential Bernoulli, energy, and rate equations implies that only two of the preceding linearizations are required, since they effectively replace the continuity and the normal momentum equations When additional linearized integrands are employed, the same number of conditions imposed by other equations must be relaxed, implying that certain equations will not be satisfied in the flow field, depending upon the scheme used This is characteristic of integral methods in which interpolation formulas are used for certain integrands The conservation equations are satisfied only on the average in the flow field but are locally satisfied at the interpolation points, in particular, at the body surface and shock for the first approximation More intermediate strips (i e , interpolation points) are required if increased accuracy is desired within the flow field

We may consider in detail one method that determines the flow-field properties along streamlines from the solution to the first approximation To trace a streamline, a mass flow balance is performed, i e , mass flow through shock between axis and streamline is set equal to mass flow between desired streamline and body surface The location of such a streamline in the shock layer for an arbitrary ξ is

$$\rho^0 q^0 (1 + \epsilon_2)^2 \sin^2\xi_2 = 2\eta\epsilon[\rho_0 u_0 + \tfrac{1}{2}\rho_1 u_1 (1 + \epsilon)\eta - \tfrac{1}{2}\rho_0 u_0 \eta] \sin\xi \quad (2\,42)$$

where subscript 2 refers to the conditions at the shock point where the streamline enters the layer, and corresponding (η,ξ) coordinates are implicit The three equations for p, ρ, u, v are

$$\rho ur = \rho_0 u_0 \sin\xi + [\rho_1 u_1 (1 + \epsilon) - \rho_0 u_0] \sin\xi \quad (2\,43)$$

$$\rho uvr = \rho_1 u_1 v_1 (1 + \epsilon) \sin\xi \quad (2\,44)$$

$$(2k^0p + \rho u^2)(1 + \epsilon\eta) \sin\xi = (2k^0p_0 + \rho_0 u_0^2) \sin\xi + [(2k^0p_1 + \rho_1 u_1^2)(1 + \epsilon) - (2k^0p_0 + \rho_0 u_0^2)]\eta \sin\xi \quad (2\,45)$$

where $r = (1 + \epsilon\eta) \sin\xi$ The differential Bernoulli equation is

$$k^0(dp/ds) + \rho q(dq/ds) = 0 \quad (2\,46)$$

in which $q^2 = u^2 + v^2$ Rate equations along streamlines are

$$\rho(u^2 + v^2)^{1/2}(dc_j/ds) = K_j \qquad (j = \mathrm{O, N, NO}) \quad (2\,47)$$

Conservation of mass requires

$$c_O + c_{O_2} + c_N + c_{N_2} + c_{NO} = 1$$

$$c_O + c_{O_2} + (M_O/M_{NO})c_{NO} = \bar{m}_O \quad (2\,48)$$

Energy and enthalpy equations are, respectively,

$$h + q^2 = 1 \quad (2\,49)$$

$$h = h(T, c_O, c_N \quad) \quad (2\,50)$$

The relation between s and ξ is

$$ds = (1 + \epsilon\eta)[1 + (v/u)^2]^{1/2} d\xi \quad (2\,51)$$

Equations (2 42–2 51) specify the flow properties including species concentrations along a streamline in the shock layer The equation of state does not appear in the set and is not necessarily satisfied as was discussed previously For equilibrium flow, the equilibrium expressions replace the rate equations (2 47)

Actual calculations were performed by using the linearized set (ρur), (ρuvr), $(k^0p + \rho u^2)r$, and $p(1 + \epsilon\eta)$ This reduced the calculation of p, ρ, u, and v to an algebraic manipulation rather than an integration as required by the Bernoulli equation The concentrations of the various species still follow upon integration of the rate equations No integrations of this type were carried out

III Numerical Problems: Results and Discussion

3 1 Numerical Problems

The equations developed in Secs 2 5 and 2 6 were programmed for an IBM 709 computer Special numerical problems in the calculations proved to be of two types: 1) those associated with integration of the differential equations of nonequilibrium flow and 2) those associated with the singular floating boundary condition that is characteristic of the integral method Specifically, the computational problems may be divided into three distinct areas: 1) along the stagnation streamline; 2) integration away from the stagnation point; and 3) continuity through the point at which $u_0^2 = k^0(dp_0/d\rho_0)$ (see Sec 2 5) The first two problem areas are associated with numerical instabilities of the equations when any of the various reactions are near equilibrium, i e , approaching equilibrium or departing from equilibrium Specifically, the rate equations are unstable unless the integration step-size is carefully controlled to maintain a bounded error This is particularly important 1) immediately behind the shock, 2) when individual reactions approach equilibrium in the shock layer, and 3) in the vicinity of the stagnation point Immediately behind the shock, the concentrations c_O, c_N, and c_{NO} are initially at very small freestream values but tend to rise very rapidly toward or even beyond their equilibrium values Step-sizes must be kept very small in this region to maintain stability As the integration proceeds toward the body along the stagnation streamline, the step-size is increased as rapidly as is consistent with the stability criteria When any reactions approach equilibrium, step-size must again be shortened in order to maintain stability It is now advantageous to replace the rate equation corresponding to the reaction in equilibrium by its corresponding equilibrium expression

It is to be noted that the equilibrium states for the different reactions are not necessarily independent, i e , certain combinations of reactions (2 15–2 20) going to equilibrium imply that the whole system will be in equilibrium This procedure is continued until all reactions are in equilibrium or until the integration approaches the stagnation point where all reactions go to equilibrium as the flow velocity approaches zero Again, the step-size must be shortened After the velocity v becomes of order 10^{-4}, a constant-pressure and enthalpy-relaxation process, as described below, yields the stagnation conditions

Although, in principle, the rate equations may be used anywhere, in practice it is preferable to continue using the equilibrium expressions for the integration process proceeding away from the stagnation point This avoids very short step-sizes required by the rate equations when near equilibrium A perturbation procedure on the equilibrium solution may then be used to determine whether or not it is appropriate to continue use of such equilibrium expressions The perturbation is introduced by arbitrarily "freezing" the equilibrium flow locally for a short distance and observing whether or not the nonequilibrium and equilibrium solutions diverge from one another If not, the equilibrium solutions are continued; otherwise, the rate equations are used

The third problem area is the usual requirement of a continuous solution at the "sonic" point by choice of the proper stagnation-point shock-standoff distance This involves some decision with regard to the smoothness with which the continuity occurs Of course, in practice, consideration of the first approximations ($N = 1$) is consistent with iterating only a few times to obtain three or four decimal-place accuracy in the standoff distance The location of the singularity is quite adequately determined

Typical run times on an IBM 709 computer for a complete solution, excluding streamline calculations as described in Sec 2 6, are on the order of 10 min for perfect gas (frozen) and identical equilibrium flows and 10–25 min for nonequilibrium flow cases

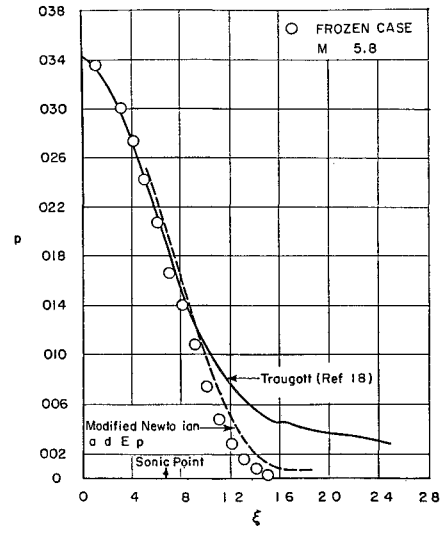

Fig 2 Pressure distribution along body surface

3 2 Results along Stagnation Streamline and Body Surface

Consideration was given the frozen (i e , perfect) gas both as a limiting case and as a check on the formulation and computational techniques by virtue of comparison with existing solutions Such a comparison with the results of Traugott[18] is shown in Fig 2 The corresponding initial shock detachment distances for the present solution and that of Ref 18 are 0 1414 and 0 1498, respectively An apparent explanation for the differences is the different choice of dependent variables in the two formulations Belotserkovskii[2] indicated previously that slightly different answers have been obtained upon using different sets of dependent variables This may be considered as an indication of the accuracy of the first approximation, since the limit of an infinite number of strips does imply a solution independent of the choice of dependent variables

A number of solutions have been completed for a range of speeds and altitudes, but only one will be presented in detail here, since there exists a solution from an inverse method[13, 17] corresponding to this particular case Results for concentrations of nitric oxide, nitrogen, and oxygen atoms and the temperature profile along the axial streamline are presented in Figs 3 and 4 for a 30-cm sphere flying at 60 96 km at a velocity of 4570 m/sec (based on 1959 ARDC atmosphere) The corresponding solution from Ref 17 as obtained by the inverse method is included for comparison An additional curve has been included on Fig 3a for the nitric oxide concentration to show the effect of excluding the bimolecular reaction (2 20) This results in a curve that is in reasonable agreement, particularly near the shock, with that of Ref 17, where the reaction has been excluded The apparent lag in the rise of the NO concentration without reaction (2 20) is a result of specifying that no dissociation occurs immediately behind the shock Since the remaining reactions involving NO all require the presence of N or O, no nitric oxide can be formed until N_2 or O_2 is dissociated The discrepancies are attributed to the difference in the gas models and methods used

In Figs 3 and 4 it appears that the temperature and concentrations do not reach their equilibrium values at the stagnation point If, however, the gas is allowed to "relax" to some equilibrium value while maintaining a constant stagnation pressure, the properties do attain values nearly equal to those of the identical equilibrium flow process This

follows, since nonequilibrium and equilibrium stagnation pressures do not differ appreciably In fact, the procedure to obtain stagnation-point conditions makes use of this constant-pressure (and enthalpy) relaxation process In principle, the stagnation-point conditions may be determined by allowing the integration along the axial streamline to proceed until the axial velocity v becomes arbitrarily small; this involves considerable and unnecessary computing time so that, in practice, integration ceased when the axial velocity became less than about 10^{-4} For cases that are far from equilibrium, this procedure may not be sufficient to reach equilibrium, and, hence, the constant-pressure (and enthalpy) relaxation process is required That this is the correct process to choose may be deduced from the differential Bernoulli equation, $k^0 dp_s = -\rho v\, dv$ The change in pressure over the small increment $d\eta$ to the stagnation point is of the order $v\, dv$; thus, if $v \sim 10^{-4}$, the change in p is 10^{-8} in the last interval, $\Delta\eta$ (similarly for enthalpy) It appears reasonable to consider p and h constant over this interval Of course, the presence of a boundary layer makes the preceding comments somewhat academic, since the conditions at the stagnation point will actually be governed by transport phenomena

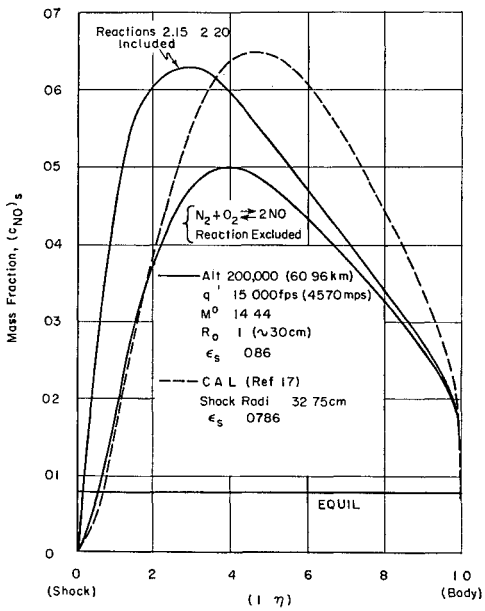

Fig 3a Stagnation streamline c_{NO} distribution

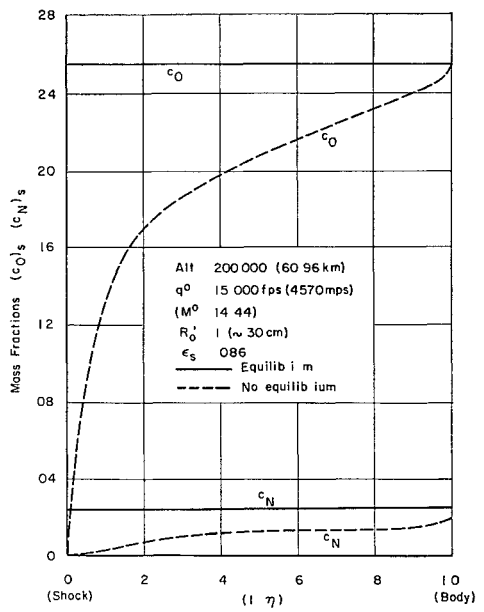

Fig 3b Stagnation streamline c_N, c_O distribution

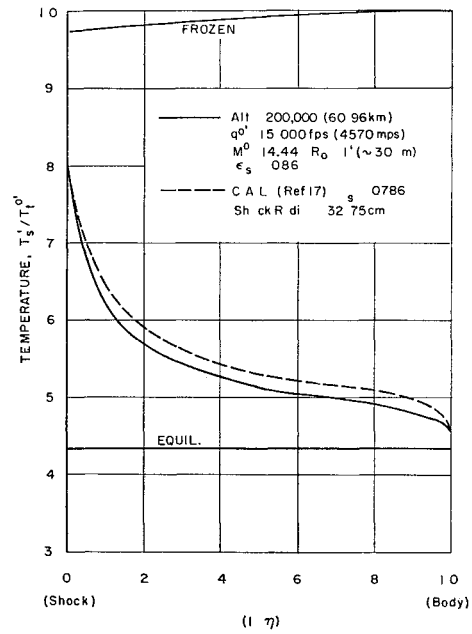

Fig 4 Stagnation streamline temperature distribution.

The frozen, equilibrium, and nonequilibrium pressure distributions along the body surface are shown in Fig 5, together with the location of the singular point As discussed earlier, this point corresponds to the sonic point for frozen and equilibrium flows, whereas in nonequilibrium flow, it represents only the location where the streamtubes have their local minimum cross-sectional area It is apparent that nonequilibrium effects on the pressure are small A good approximation for the pressure distribution is found to be given by the so-called modified Newtonian formula with the Busemann centrifugal correction term included:

$$\frac{p_0}{p_t^0} = \frac{p_{0s}}{p_t^0} - \frac{4}{3}\left(\frac{p_0}{p_t^0} - \frac{p^0}{p_t^0}\right)\sin^2\xi \qquad (3\,1)$$

This is also shown on Fig 5 for the frozen case For large M^0, (3 1) gives the result that $p_0 \to 0$ at $\xi = 60°$ (neglecting p^0) The present solutions also yield zero pressure on the body surface, although they are at a larger value of $\xi(\approx 70°)$ for frozen, equilibrium, and nonequilibrium flows This is

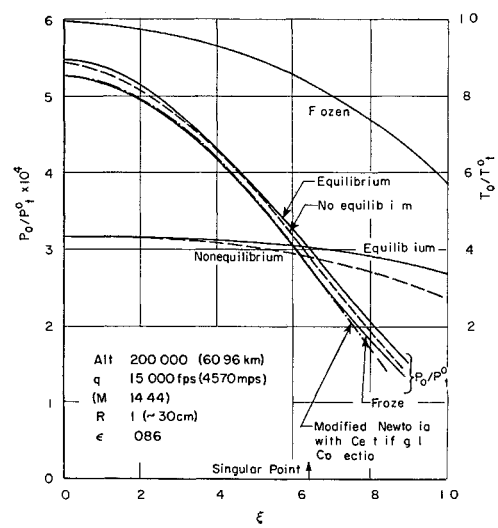

Fig 5 Pressure and temperature distributions along body surface

Table 1 Tabulation of cases as shown in Figs 8a and 8b

Case	Alt, km	M^0	a^0, mps	$q^{0\prime}$, mps	R_0', m	$\rho^{0\prime}$, kg/m^3	$T^{0\prime}$ K	Comments
1	60 96	14 441	316 50	4570 58	3×10^{-1}	3 1384 $\times 10^{-4}$	249 3	to check, Ref 17
2	10	10	299 53	2995 3	1 0	4 1351 $\times 10^{-1}$	223 26	nonequil
3	10	15		4492 95	10^{-1}			equil [c](1)[b]
4	30	15	304 83	4572 45	10^{-2}	1 7861 $\times 10^{-2}$	231 24	nonequil [a] (1)
5	30	15		4572 45	10^{-1}			near equil (1)
6	30	25		7620 75	10^{-2}			equil [a] (1) (2)
7	50	20	337 03	6740 6	3×10^{-1}	1 0829 $\times 10^{-3}$	282 66	near equil [d] (1)
8	50	20		6740 6	10^{-4}			near froz [d] (1)
9	50	25		8425 75	2 13 $\times 10^{-2}$			near equil (2)
10	70	25	290 22	7255 5	3×10^{-1}	1 0008 $\times 10^{-4}$	209 59	near equil [e] (1)[d] (2)
11	70	25		7255 5	10^{-2}			nonequil [c] [d] (2)
12	70	25		7255 5	10^{-3}			near froz [d] (2)

[a] Effect of changing M^0 for same R_0 and altitude
[b] Numbers in parentheses refer to corresponding cases to be compared; e g compare cases 3 and 5 for c effect; compare cases 6 9 and 11 also for c effect but for different R_0 and M^0
Effect of changing altitude (and velocity) for same R_0 and M^0
[d] Effect of changing R_0 for same M^0 and altitude
Effect of changing M^0 and altitude for same body

well past the sonic point, beyond which the method of characteristics may be employed

The temperature variations along the body surface are also shown in Fig 5 Energy released because of recombinations counteracts the temperature drop due to the flow expansion around the body, and, consequently, the equilibrium and nonequilibrium curves are flatter than the frozen temperature variation Similarly, recombination rates in the nonequilibrium case are not sufficiently rapid, in comparison with the identical equilibrium case, to overcome the temperature drop due to the flow expansion

Figure 6 clearly shows the effects of finite rate processes on the concentrations of nitric oxide and atomic oxygen and nitrogen along the body surface

3 3 Shock Shape, Shock Detachment Distance, and Singular Point Location

Typical shock shapes for frozen, nonequilibrium, and equilibrium flow are shown in Fig 7 As one would expect, the higher densities for the latter two cases cause the shocks to be displaced a lesser distance from the body than in the frozen-flow situation

For certain approximate solutions of the blunt-body problem, the shock is assumed to be concentric with the body; thus, only the initial shock detachment distance at the axis of symmetry is required For frozen flow, the normalized detachment distance, measured in units of body radius, is only a function of the freestream Mach number and ratio of specific heats γ^0 The normalized stagnation detachment distance is plotted in Fig 8 for all frozen, nonequilibrium, and identical equilibrium cases as tabulated in Table 1 The agreement of the frozen cases with experiment[19] at the lower Mach numbers (<5) is excellent, but at higher Mach numbers the limiting value does not approach the value of ~0 14 as predicted by the "exact" calculations of Van Dyke [8]

The 12 nonequilibrium cases in Fig 8a represent the entire spectrum from near-equilibrium to near-frozen flow for an inviscid shock layer Of course, at altitudes above 50 or 60 km, a purely inviscid calculation may not be realistic,

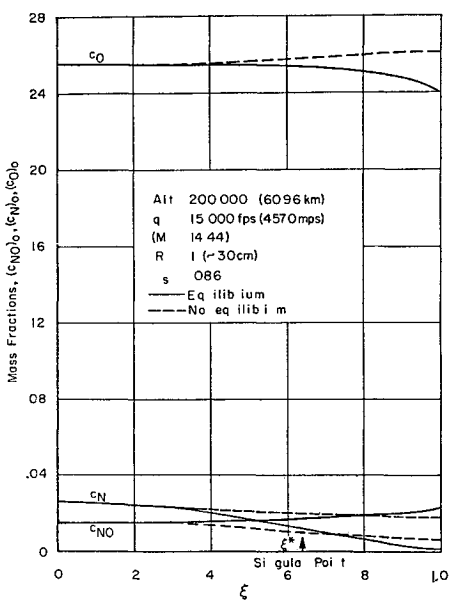

Fig 6 c_{NO}, c_O, c_N distribution along body surface

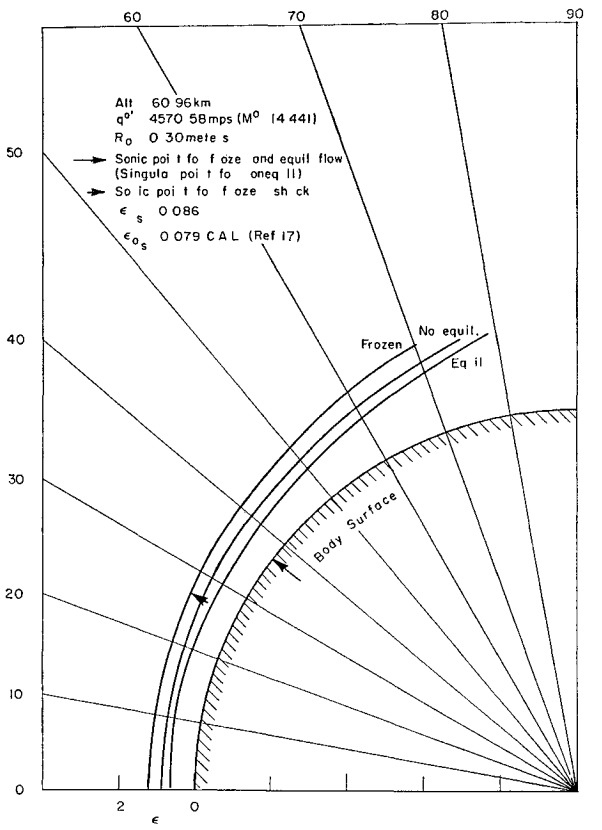

Fig 7 Shock shape

since the boundary layer becomes rather thick and does influence the inviscid flow field

The stagnation detachment distance for these cases appears, however, to be rather insensitive to the degree of departure from equilibrium This result is apparently a defect of the first approximation when considering the extreme cases of near-frozen or near-equilibrium flow Regardless of what is actually happening in the shock layer (excluding the stagnation streamline), the first approximation can only account for variations due to changes at the shock and body surface If these changes are insensitive to scale variations, then they cannot appreciably affect the average properties such as the detachment distance In fact, for given free-stream conditions, the properties immediately behind the shock and the equilibrium conditions at the stagnation point are relatively insensitive to a change in length scale Higher approximations are required to account properly for the rapid behavior of flow properties near the shock or body for near-equilibrium or near-frozen flows, respectively One does anticipate a continuous variation of the detachment distance from the frozen to equilibrium values as the reaction rates (scale) are increased

Location of the singular point is shown in Fig 8b The result for frozen flow is plotted as the solid curve As discussed previously, the singular point of the present analysis corresponds to the sonic point in both frozen and equilibrium flows Experimental sonic points as determined by Kendall[19] are also included The disagreement is about 6% at $M^0 = 4\ 76$ Figure 8b indicates that the present solutions give a limiting sonic location of approximately 0 64 rad from the axis of symmetry as the freestream Mach number increases to extreme values If Eq (3 1) is multiplied by $p_t{}^0/p_{0s}$ and the term p^0/p_0 of order $(M^0)^{-2}$ is ignored for very large M^0, the ratio of surface to stagnation-point pressure is

$$p_0/p_0 = 1 - \tfrac{4}{3}\sin^2\xi \qquad (3\ 2)$$

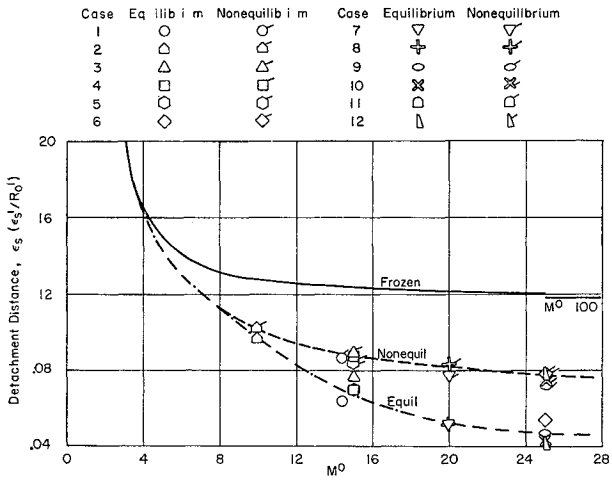

Fig 8a Shock detachment distance along axis of symmetry

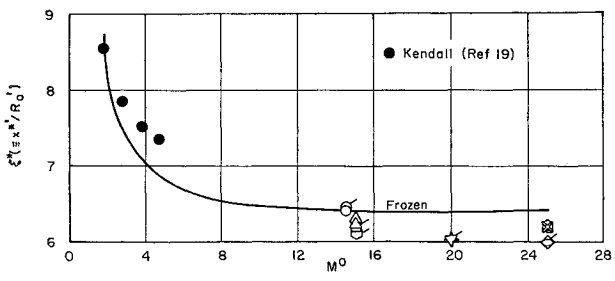

Fig 8b Singular point (sonic point for frozen and equilibrium flow) location

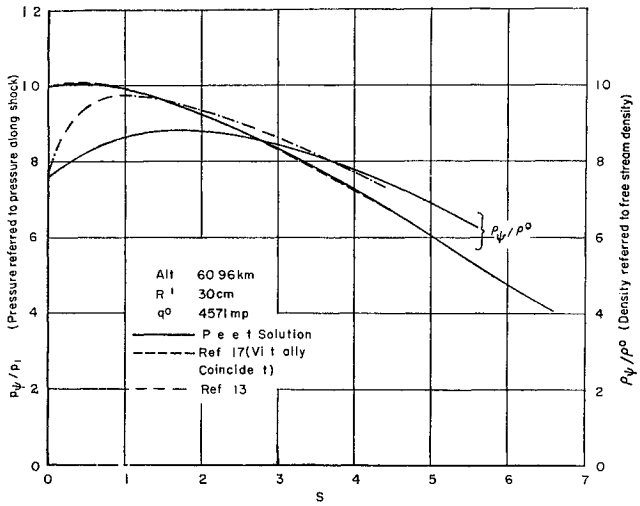

Fig 9 Pressure and density variations along 9° streamline in terms of distance along streamline

At the sonic point (perfect-gas or frozen flow), $p_0{}^*/p_{0s} = 0\ 528$, this implies that $\xi^* = 0\ 64$ is in agreement with the present solutions The corresponding points for equilibrium and nonequilibrium flows do not deviate appreciably from the frozen results

3 4 Flow-Field Calculations

As discussed earlier, the properties in the shock layer, aside from those immediately behind the shock and along the axial streamline and body surface, may be calculated from the solutions for the first approximation by a streamline technique Calculations for the frozen and equilibrium flows may be reduced to algebraic manipulations, whereas the rate equations must be integrated in nonequilibrium flows It is possible, however, to determine the pressure, density, and velocities along the streamlines for all three cases if the set (ρur), (ρuwr), $(k^0p + \rho u^2)r$, and $p(1 + \epsilon\eta)$ is linearized across the shock layer (see Sec 2 6) without integration But again, integration of the rate equations is required for nonequilibrium flow in order for temperatures and the concentrations to be determined In Fig 9, the variations of the pressure (normalized with respect to that at the shock) and the density (normalized by the freestream density) along a streamline that enters the shock at 9° off the axis of symmetry is plotted as a function of s, the normalized streamline distance measured from the shock The agreement with Refs 13 and 17 is very good in view of the approximations made in the present formulation Unfortunately, streamline integrations for the concentrations were not performed

3 5 Concluding Remarks

A direct solution to the blunt-body problem using the method of integral relations has been completed For the first approximation, no additional assumptions beyond those already made for the perfect-gas problem are required In principle, only an additional statement as to the conservation of each reacting species and a detailed description of the gas medium are required for the nonequilibrium problem Solutions for the flow of a five-component dissociating gas about a sphere have been presented for the first approximation These yield concentrations and temperatures only immediately behind the shock, along the axial streamline, and on the body surface It is possible, however, to determine these properties in the flow field by performing a streamline calculation in conjunction with the solutions from the first approximation The latter gives streamline locations and the variations of pressure, density, and velocity along the streamline

References

[1] Dorodnitsyn, A A, "A contribution to the solution of mixed problems of transonic aerodynamics," *Advances in Aeronautical Sciences* (Pergamon Press, New York, 1959), Vol 2, pp 832–844

[2] Belotserkovskii, O M "Flow past a circular cylinder with a detached shock wave," Avco-RAD 9-TM59-66 (September 30, 1959)

[3] Hayes W and Probstein, R, *Hypersonic Flow Theory* (Academic Press, New York, 1959), Chaps 3–6

[4] Freeman, N C Nonequilibrium flow of an ideal dissociating gas, J Fluid Mech **9**, 407–425 (1958)

[5] Ellington, D, "Approximate method for hypersonic nonequilibrium blunt body airflows," AIAA J **1**, 190 (1963)

[6] Maslen, S H and Moeckel, W E, "Inviscid hypersonic flow past blunt bodies," J Aerospace Sci. **24**, 683–693 (1957)

[7] Gravalos, F G, "Supersonic flow about a blunt body of revolution, *Advances in Aeronautical Sciences* (Plenum Press, New York, 1957), Vol 2, Paper 5

[8] Van Dyke, M D, "The supersonic blunt body problem—review and extensions," J Aerospace Sci **25**, 485–496 (1958)

[9] Garabedian, P R and Lieberstein, H M, "On the numerical calculation of detached bow shock waves in hypersonic flow, J Aerospace Sci **25**, 109–118 (1958)

[10] Gravalos F G, Edelfelt, I H, and Emmons H W, "The supersonic flow about a blunt body of revolution for gases at chemical equilibrium, *IX Astronautical Congress* (Springer-Verlag, Berlin, 1959) pp 312–332

[11] Lick, W, "Inviscid flow around a blunt body of a reacting mixture of gases, Part A General analysis," Rensselaer Polytechnic Institute, TRAE 5810 (May 1958)

[12] Lick, W, "Inviscid flow around a blunt body of a reacting mixture of gases Part B Numerical solutions," Rensselaer Polytechnic Institute, TRAE 5814 (December 1958)

[13] Hall J G, Eschenroeder, A Q, and Marrone, P V, "Inviscid hypersonic air flows with coupled chemical reactions," J Aerospace Sci **29**, 1038 (1962)

[14] Bauer, S H and Tsang, S C, "Mechanisms for vibrational relaxation at high temperatures," Phys Fluids **6**, 182–189 (1963)

[15] Treanor, C E and Marrone, P V, "Vibration and dissociation coupling behind strong shock waves," *Proceeding of the U S A F Symposium of Dynamics of Manned Lifting Planetary Entry* (John Wiley and Sons, New York, 1963), pp 160–171

[16] Marrone, P V and Treanor, C E, "Chemical relaxation with preferential dissociation from excited vibrational levels," Phys Fluids **6**, 1215 (1963)

[17] Gibson, W E and Marrone, P V, "A similitude for nonequilibrium phenomena in hypersonic flight," AGARD Meeting on High Temperature Aspects of Hypersonic Fluid Dynamics, Brussels, Belgium (March 1962)

[18] Traugott, S C, "An approximate solution of the supersonic blunt body problem for prescribed arbitrary axisymmetric shapes, J Aerospace Sci **27**, 361–370 (1960)

[19] Kendall, J M, Jr, "Experiments on supersonic blunt-body flows," Jet Propulsion Lab Progress Rept 20 372 (February 27, 1962)